Homogeneous Catalysis. Mechanism of Catalytic Hydroacylation: The Conversion of 4-Pentenals to Cyclopentanones

David P. Fairlie and B. Bosnich*

The Lash Miller Chemical Laboratories, University of Toronto, 80 St. George Street, Toronto, Ontario, Canada M5S 1A1

Received October 30, 1987

The mechanism of catalytic hydroacylation of 4-pentenal to cyclopentanone using the catalysts [Rh(diphos)]$^+$ and [Rh((*S*,*S*)-chiraphos)]$^+$ has been investigated by multinuclear NMR spectroscopy. The catalytic precursors exist as arene-bridging dimers, [Rh(diphosphine)]$_2^{2+}$, in CH_3NO_2 solutions. These dimers are not catalytically active and require to be split by the substrate before catalysis occurs. The [Rh(diphos)]$_2^{2+}$ dimer exists as two isomers; the minor isomer reacts with the substrate approximately 100 times faster than the major isomer. Numerous rapidly equilibrating catalyst–substrate adducts are observed. Most of these species are catalytically inactive, but they do affect both the turnover rate and the turnover number. The higher the ratio of substrate to catalyst, the slower the turnover rate but the higher the turnover number. This substrate inhibition of rate appears to be related to the catalyst being tied up as catalytically unproductive adducts, and the extension of the turnover number is due to suppression of decarbonylation by substrate interaction. The species [Rh(diphosphine)(ketone)(CO)]$^+$ is found to rapidly decarbonylate 4-pentenal and gives rise to low turnover numbers in acetone solution as well as product inhibition in non-ketonic solvents. No catalytic intermediates were identified. Deuterium-labeling studies reveal that the C–H activation, hydride transfer to the double bond, and carbonyl deinsertion are all fast and reversible steps. The turnover limiting step is the irreversible reductive elimination from a metallocyclohexanone to produce cyclopentanone. The kinetics of catalysis are such that, at any stage of catalysis, most of the material lies outside of the catalytic cycle.

The preceding paper[1] describes the development of a series of catalysts of the type [Rh(diphosphine)]$^+$ which convert 4-pentenals to cyclopentanones by intramolecular cyclization. Because the net process involves the addition of the aldehyde hydrogen atom and the carbon atom of the acyl group to the double bond, it is referred to as hydroacylation (eq 1). Although remarkably facile when

(1)

these new catalysts are used, hydroacylation is clearly a complex multistep process.

Miller[2] has previously investigated some of the mechanistic aspects of hydroacylation using the marginally catalytic species [Rh(PPh$_3$)$_3$Cl], and his work suggested the broad outlines of the mechanism for this particular catalyst. Miller determined the fate of the deuterium label in the substrate CH_2=$CHCH_2CH_2CDO$ for the cyclization process. He found that the deuterium label appeared mainly in the expected β-position of the cyclopentanone product but also some 10% of the deuterium was located at the α-position of the product. On the basis of this and the known behavior of rhodium(I) complexes, he proposed the hydroacylation mechanism outlined in Figure 1 for the [Rh(PPh$_3$)$_3$Cl] complex.

The first step involves oxidative addition of the aldehyde C–H bond to rhodium(I), a process implicated in the decarbonylation of aldehydes[3] and demonstrated by the characterization of the hydrido–acyl species **2** in two separate systems,[4] one of which involved 4-pentenal.[5] Hydride addition to a double bond (**2** → **3**) is well-known, and the reductive elimination step (**3** → **7**) is implicated by the result. In addition to this direct pathway, the appearance of **8** implies the formation of the five-membered metallacycle **4** which upon β-elimination gives **5** which collapses to **8** via **6**.

The mechanism outlined in Figure 1 for the [Rh(PPh$_3$)$_3$Cl] complex provides the basis for our analysis of the mechanism of hydroacylation with the [Rh(diphosphine)]$^+$ catalysts for it allows us to consider specific steps of the mechanism. We begin by considering the interaction of the substrate with the rhodium(I) complex before oxidative addition occurs. This interaction is complex, affects the rate of catalysis, determines the distribution of side products, and is germane to establishing the catalytically active species.

Substrate–Catalyst Interaction

For the purpose of investigating the catalyst–substrate interaction, we have chosen to concentrate mainly on the [Rh(diphos)]$^+$ (diphos = $(C_6H_5)_2P(CH_2)_2P(C_6H_5)_2$) catalyst and its catalytic conversion of the parent substrate, 4-pentenal. As determined in the previous paper[1] this catalyst exists mainly as the disolvento monomer, [Rh(diphos)(acetone)$_2$]$^+$, in dilute acetone solutions, probably as the perchlorato monomer, [Rh(diphos)(ClO$_4$)], in CH_2Cl_2 solutions, and as the arene-bridging dimer **9**, in CH_3NO_2

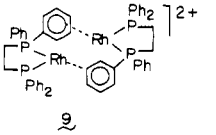

9

solutions. Although the catalyst was found to exist as the meso dimeric isomer in the solid state,[6] it exists as two

* To whom correspondence should be addressed at the Department of Chemistry, The University of Chicago, 5735 South Ellis Avenue, Chicago, Illinois, 60637

(1) Fairlie, D. P.; Bosnich, B. *Organometallics*, preceding paper in this issue.
(2) Lachow, C. F.; Miller, R. G. *J. Am. Chem. Soc.* **1976**, *98*, 1281. Campbell, R. E.; Lachow, C. F.; Krishnakant, P. V.; Miller, R. G. *Ibid.* **1980**, *102*, 5824. Campbell, R. E.; Miller, R. G. *J. Organomet. Chem.* **1980**, *186*, C27.
(3) Tsuji, J.; Ohno, K. *Tetrahedron Lett.* **1965**, 3669.
(4) Suggs, J. W. *J. Am. Chem. Soc.* **1978**, *100*, 640.
(5) Milstein, D. *J. Chem. Soc., Chem. Commun.* **1982**, 1357.

0276-7333/88/2307-0946$01.50/0

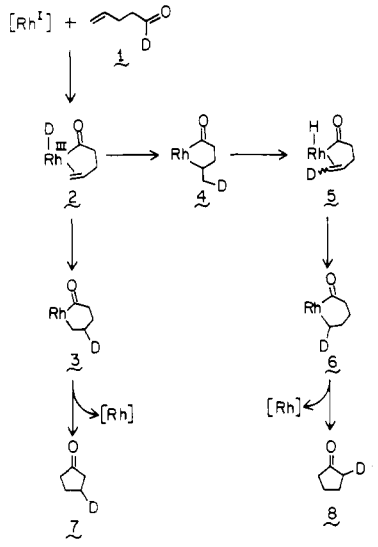

Figure 1. Outline of the proposed mechanism of hydroacylation of 4-pentenal using the $[Rh(PPh_3)_3Cl]$ complex.

isomers in the ratio of 7:1 in CH_3NO_2 solutions which we ascribe[1] to the meso and racemic forms of the dimer. Although we have not established the fact, there is circumstantial evidence suggesting that the major isomer is the meso form. For reasons of solubility most ^{31}P NMR data were collected in nitromethane solutions.

The first question we address is whether the dimer itself or a substrate–catalyst adduct monomer is the catalytically active species. Our evidence against the dimer being the catalytically active species is indirect. We note that the dimer is a coordinatively saturated 18-electron species which therefore is not expected to engage in oxidative addition. This is consistent with our observation that the $[Rh(diphos)PhBPh_3]$ complex[7] containing a more firmly bound π-phenyl group is catalytically inactive. Also the 16-electron dimer $[Rh(diphos)Cl]_2$ is only marginally catalytic[1] at least partly due to the requirement that the dimer be split by the substrate before catalysis can occur. Finally, the turnover rates for 4-pentenal are similar in acetone, CH_3NO_2, and CH_2Cl_2 solutions, despite the different forms of the catalyst, suggesting a common catalytically active species in all three solvents. All of these observations strongly imply that the dimer is not catalytically active.

If the dimer is not catalytically active, then what is the nature of the catalytically active species? It is clearly a catalyst–substrate adduct, but we have not been able to identify it in the preequilibrium to the catalytic cycle because we suspect that it is highly reactive and does not accumulate. The following experiments were carried out at $[Rh] \approx 10$ mM. Addition of 10 equiv of 4-pentenal to a CH_3NO_2 solution of the dimer at −30 °C leads to the "instantaneous" loss of ^{31}P NMR peaks associated with the minor isomer; the major isomer dimer then decays at a rate of at least 10^2 times more slowly. This marked contrast in behavior of the two dimer isomers establishes that the two are not in rapid equilibrium. No catalysis is observed at −30 °C; slow catalysis only sets in at around 0 °C. Addition of 100 equiv of 4-pentenal to a CH_3NO_2 solution of the dimer at 5 °C leads to the same sequential loss of the minor and major isomers, but because the overall splitting process is faster at 5 °C than at −30 °C and the catalysis is slow, we were able to observe a variety of substrate–catalyst species by ^{31}P NMR. The only species we were able to identify with certainty was the $[Rh(diphos)(CO)_2]^+$ ion which results from decarbonylation during catalysis. The ^{31}P NMR spectra encompassed resonances in regions characteristic of olefin and oxygen binding to $[Rh(diphos)]^+$. As the catalysis proceeds at 5 °C, all the ^{31}P NMR peaks corresponding to the substrate–catalyst adducts decrease roughly synchronously. If 500 equiv of 4-pentenal are added, essentially the same ^{31}P NMR peaks are observed but in different proportions. These, too, decay syncronously as catalysis proceeds. The many substrate–catalyst adducts that are observed during catalysis may arise from interaction of the substrate either with the $[Rh(diphos)]^+$ complex or with intermediates in the catalytic cycle or both.

As we describe in the next section, the catalysis is inhibited by substrate, the more substrate that is added the slower the catalysis. This substrate inhibition is consistent with the notion that the catalyst is deactivated by being tied up as catalytically unproductive adducts that inhibit the formation of the catalytically active species.

We believe that the catalytically active preequilibrium species resembles the chelating substrate adduct **10**. That

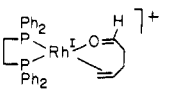

10

10 is likely to be a stable (although reactive) structure is demonstrated by the observation that when 1 equiv of the ketone **11** analogous to 4-pentenal is added to a CH_3NO_2 solution of the dimer, a dimer splitting reaction occurs; first the minor isomer decays followed, more slowly, by the major isomer to give a single species, the ^{31}P NMR spectrum of which is consistent with a structure analogous to **10**. Even in 500 equiv of ketone **11** are added, only the chelating adduct is observed, attesting to its stability.

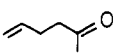

11

Substrate Inhibition

Because of the inherent complexity of hydroacylation arising from the numerous catalyst–substrate adducts, substrate decarbonylation, and the different splitting rates of the two diastereomers in CH_3NO_2 solutions, we were unable to obtain useful rate constants for catalysis. The relative catalytic rates, however, can be seen clearly from the plot of percent conversion of substrate with time. In Figure 2 we plot the percent conversion of 4-pentenal by using the $[Rh(diphos)]^+$ catalyst in CH_3NO_2 solutions at 30 °C for various ratios of substrate to rhodium. The conversion was followed by ^1H NMR. In all cases the concentration of rhodium is about 10 mM. It will be seen that as the amount of substrate is increased at constant rhodium concentration, the catalytic rate slows down. We should point out that at high substrate to rhodium ratios the solutions are not dilute; for example at a 300:1 ratio approximately equal volumes of 4-pentenal and CH_3NO_2 are used. These results are clearly consistent with our earlier assertion that, with increasing concentrations of substrate, the catalyst is increasingly tied up as catalytically unproductive substrate–catalyst adducts. Since many of these adducts undoubtedly involve rhodium–olefin binding, it follows that the addition of a different olefin to the catalytic solution should slow down catalysis by

(6) Halpern, J.; Riley, D. P.; Chan, A. S. C.; Pluth, J. J. *J. Am. Chem. Soc.* **1977**, *99*, 8055.

(7) Albano, P.; Aresta, M. *J. Organomet. Chem.* **1980**, *190*, 243.

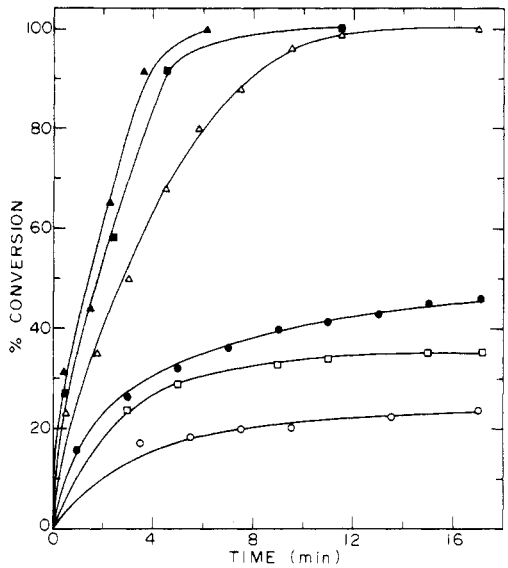

Figure 2. A plot of percent conversion of 4-pentenal to cyclopentanone versus time at 30 °C using the [Rh(diphos)]$^+$ catalyst at constant concentration of [Rh] = 10 mM and varying concentrations of substrate in CD_3NO_2 solutions. The ratios are as follows: ▲, 33:1; ■, 51:1; △, 111:1; ●, 190:1; □, 271:1; ○, 436:1 ([substrate]:[Rh]).

adduct formation. This is so. Using a 100:1 substrate:Rh ratio in the presence of 500 equiv of 1-pentene in CH_3NO_2 slows the catalysis by at least a factor of 5. Similarly it follows that with increasing dilution for a constant substrate:Rh ratio the catalytic rate should increase because dilution should decrease the population of the rapidly equilibrating adducts. We find this to be the case. With use of 200:1 substrate:Rh ratio, a twofold and a threefold dilution caused successive (30%) increases in the turnover rate. Thus there seems little doubt that the origin of the substrate inhibition resides in the formation of catalytically unproductive substrate–catalyst adducts.

If the efficiency of the catalyst is defined in terms of both turnover rate and turnover number, substrate inhibition effects a trade-off between these two quantities. We find that although with increasing substrate concentration the catalytic turnover rate decreases, the turnover number increases (Figure 2). That is, the rate of decarbonylation of the substrate decreases with increasing substrate concentration. Thus at 1 mM [Rh], for example, with 130:1 ratio of substrate to catalyst the substrate is fully consumed and generates 1 equiv of catalytically inactive [Rh(diphos)$(CO)_2$]$^+$ in CH_3NO_2 solutions, but a 250:1 ratio also fully consumes the substrate and generates 1 equiv of [Rh(diphos)$(CO)_2$]$^+$. That this apparently paradoxical result is connected with the initial concentration of the substrate is demonstrated by the observation that after 100 turnovers using 100:1 ratio under the above conditions, the addition of a further 150 equiv of substrate only produces a further 30 turnovers before the catalyst is fully carbonylated. The relationship between the initial ratio of substrate to rhodium and the ratio of cyclopentanone to olefin products is shown in Figure 3. The amount of non-aldehyde olefins was measured by GC, and it was shown by ^{31}P NMR of the [Rh(diphos)$(CO)_2$]$^+$ complex[1] that the amount of carbon monoxide was equal to the amount of olefin, as expected since decarbonylation of the substrate gives olefin plus CO. The plot (Figure 3) gives a straight line within experimental error. It shows that the turnover number increases as the substrate concentration is increased. This plot includes data for constant rhodium concentrations with varying substrate ratio

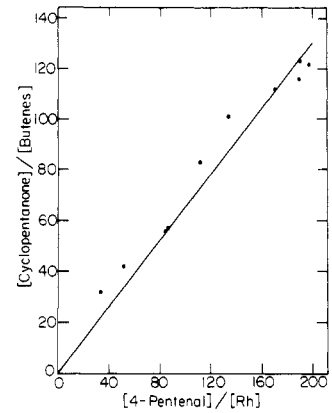

Figure 3. A plot of the ratio of cyclopentanone/butenes versus the substrate/catalyst ratio. The catalysis was carried out in CD_3NO_2 solutions at 30 °C.

and for constant [substrate]:[Rh] ratios but where the solutions were diluted (see Table I).

This extension of the life of the catalyst is reminiscent of Miller's[2] observation that ethylene increases the turnover number of the [Rh$(PPh_3)_3$Cl] catalyst. Miller presented evidence for the incorporation of ethylene in the catalytic intermediates which he suggested suppressed decarbonylation. We similarly propose that decarbonylation inhibition occurs by the intervention of a second substrate molecule in a catalytic intermediate. We propose that the intermediate **12** is responsible for suppressing

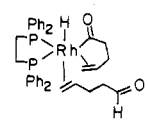

12

decarbonylation because its six-coordinate structure is expected to inhibit the process. We have no evidence as to whether the second substrate molecule intervenes at the beginning of the catalytic cycle or intercepts an intermediate at a later stage.

Catalyst Carbonylation

When CO is added to the [Rh(diphos)]$^+$ catalyst in CH_3NO_2 and in acetone solutions ([Rh] ≈ 10 mM), the CO binding is distinctly different. In CH_3NO_2 solutions the reaction with CO is slow because of the slow splitting of major dimer isomer. The only species detected is [Rh(diphos)$(CO)_2$]$^+$. When less than stoichiometric amounts of CO are added, the solution contains only the dimer and the dicarbonyl complex and no monocarbonyl species is detected by ^{31}P NMR. In acetone solutions, addition of 1 equiv of CO gives predominantly the [Rh(diphos)(CO)(acetone)]$^+$ complex, and, upon addition of a second equivalent or an excess of CO, the [Rh(diphos)$(CO)_2$]$^+$ complex is formed. When 1 equiv of CO is added to a CH_3NO_2 solution of [Rh(diphos)]$^+$ containing 50 equiv of either cyclopentanone or acetone, the monocarbonyl species [Rh(diphos)(CO)(ketone)]$^+$ is produced. This same species is formed by disproportionation of equivalent amounts of [Rh(diphos)]$^+$ and [Rh(diphos)$(CO)_2$]$^+$ induced by the addition of 50 equiv of either ketone in CH_3NO_2 solution.

We find that neither the [Rh(diphos)$(CO)_2$]$^+$ nor the [Rh(diphos)(CO)(ketone)]$^+$ species are catalysts for hydroacylation of 4-pentenal in either CH_3NO_2 or acetone solutions at 20 °C. We note, however, that in CH_3NO_2 solutions the [Rh(diphos)$(CO)_2$]$^+$ complex with 100–500 equiv of 4-pentenal causes no turnover during several hours

at 20 °C, but then a very slow turnover sets in and continues for at least 1 week. This slow turnover, we believe, is due to substrate-induced dissociation of the CO ligands.

Although the [Rh(diphos)(CO)(ketone)]$^+$ species are not catalysts for hydroacylation of 4-pentenal, they do decarbonylate 4-pentenal within a few minutes at 20 °C. Hydroacylation therefore is subject to a form of indirect product inhibition in CH_3NO_2 solutions. Hydroacylation produces both cyclopentanone and CO so that at certain stages of catalysis the [Rh(diphos)(CO)(cyclopentanone)]$^+$ species will form. Given that this species causes decarbonylation at a rate comparable to hydroacylation, its presence during catalysis will reduce both the rate and turnover number by generating the dicarbonylated catalyst. Similarly, the low turnover number (~40) for catalysis in acetone solutions is probably due to the presence of the [Rh(diphos)(CO)(acetone)]$^+$ species, which is catalytically inactive but which decarbonylates the substrate.

We find another manifestation of this form of inhibition. Thus with use of a constant concentration of the [Rh(diphos)]$^+$ catalyst ([Rh] = 3 mM), and 100 equiv of 4-pentenal in CH_3NO_2 solution, the addition of either $^1/_2$, 1, or 2 equiv of the inactive [Rh(diphos)$(CO)_2$]$^+$ species causes a successive decrease in both the turnover rate and turnover number. Since the concentration of the active catalyst is the same in all cases, the progressive reduction of the catalytic efficiency is likely due to substrate and product-induced disproportionation of the [Rh(diphos)]$^+$ and the inactive [Rh(diphos)(CO_2)]$^+$ species into catalytically inactive monocarbonyl complexes.

Finally, the [Rh(diphos)]$^+$ catalyst is a poor decarbonylating agent for aliphatic aldehydes. Addition of pentanal to either CH_3NO_2 or acetone solutions of [Rh(diphos)]$^+$ at 20 °C causes no decarbonylation of the aldehyde over several hours. The solutions require to be heated at 60 °C for several hours before detectable decarbonylation is observed. This observation is consistent with our earlier contention[1] that the binding of the olefin group of 4-pentenals will enhance the rate of C–H activation through proximal assistance.

The "Black Box" Problem

We have attempted to detect intermediates in the catalytic cycle at low temperatures in CH_3NO_2 solutions. At −30 °C ([Rh] = 10 mM) no catalysis is observed after several hours, and it is only at 0 °C that slow catalysis sets in. Using 1:1 to 100:1 ratios of substrate to catalyst, we were unable to detect any species that could be clearly identified as a putative catalytic intermediate. Neither metal–hydride signals nor proton or carbon NMR signals indicating metal–carbon bonds could be detected among signals of the substrate, product, and catalyst. It thus appears that once the appropriate substrate–catalyst adduct enters the catalytic cycle the subsequent catalytic steps have rate constants such that none of the catalytic material builds up sufficiently to be detected.[8] Thus the catalysis is a "black box" into which material enters and products emerge, but the steps in the transformation are hidden. Since we cannot "see" into the "black box", we infer the mechanism by indirect means. We chose deuterium-labeling studies.

Deuterium-Labeling Studies

The deuterium-labeling experiments were designed to address the following questions which are implicit in the proposed mechanism outlined in Figure 1. First, is the C–H oxidative addition step (**1** → **2**) reversible? Second, does hydride transfer occur to generate the five-membered metallacycle (**2** → **4**), and, if so, what is the fate of **4**? Third, is the step involving the formation of the six-membered metallacycle (**2** → **3**) reversible? Fourth, at what step(s) does decarbonylation occur to produce the carbonylated catalyst and the butene side products? Fifth, does reversible carbonyl deinsertion and insertion occur at the six-membered metallacycle **3**? Sixth, which step is the turnover limiting step?[9] Since none of the intermediates has been detected, the answers to these questions have to be inferred from the location of the deuterium label of material that emerges from the "black box".

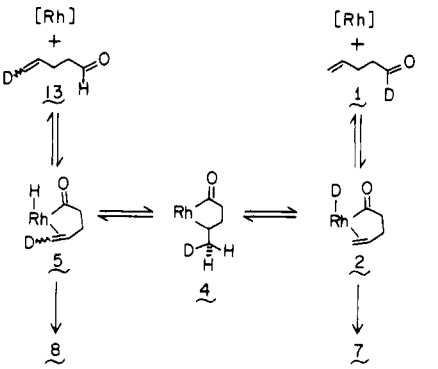

Figure 4. The proposed mechanism for deuterium transfer in catalytic hydroacylation of CH_2=$CHCH_2CH_2CDO$ using the [Rh(diphos)]$^+$ catalyst. The positive charge of the rhodium species has been omitted, and all coordinatively unsaturated species shown in the diagram may contain either bound solvent or substrate molecules.

Using the [Rh(diphos)]$^+$ catalyst in CD_3NO_2 solution and 100 equiv of the monodeuteriated 4-pentenal, CH_2=$CHCH_2CH_2CDO$, results in a catalytic rate which is about half as fast as for the undeuteriated substrate. When the catalysis is followed by ^{1}H NMR a proton signal corresponding in chemical shift to the *aldehyde* proton signal of 4-pentenal is observed; it initially increases in intensity and then decays as the catalysis proceeds. Furthermore, the cyclopentanone product contains deuterium in both the α-position **8** and the β-position **7** but the ratio (**7**:**8**) varies during the reaction. At the end of the reaction the ratio of **7**:**8** is 2.7:1 although at the early stages of catalysis this ratio can be as high as 20:1. All of these observations are independent of the initial substrate concentration used in catalysis. No H/D exchange is observed between the substrate and solvent, and the same results are observed in CD_2Cl_2 solution. Mass spectrometry shows that the cyclopentanone products incorporate one deuterium per molecule. This result demonstrates that the deuterium relocation is an intramolecular process because an intermolecular process would lead to at least double deuterium incorporation.

These results are consistent with the operation of the steps shown in Figure 4. The transfer of the deuterium from its position in **1** to the position in **13** suggests the formation of **2** followed by deuteride transfer to the olefin to give **4** which, depending on whether β-elimination involves abstraction of a hydrogen atom or a deuterium atom, gives **5** or **2**, respectively. Since as we show presently, we observe **13** during catalysis, all of the steps connecting **1**, **2**, **4**, **5**, and **13** must be reversible. In principle these steps could lead to an equilibrium mixture of **1** and **13** were

(8) *Asymmetric Catalysis*; Bosnich, B., Ed.; Martinus Nijhoff Publishers: Boston, 1986.

(9) Mackenzie, P. M.; Whelan, J.; Bosnich, B. *J. Am. Chem. Soc.* **1985**, *107*, 2046.

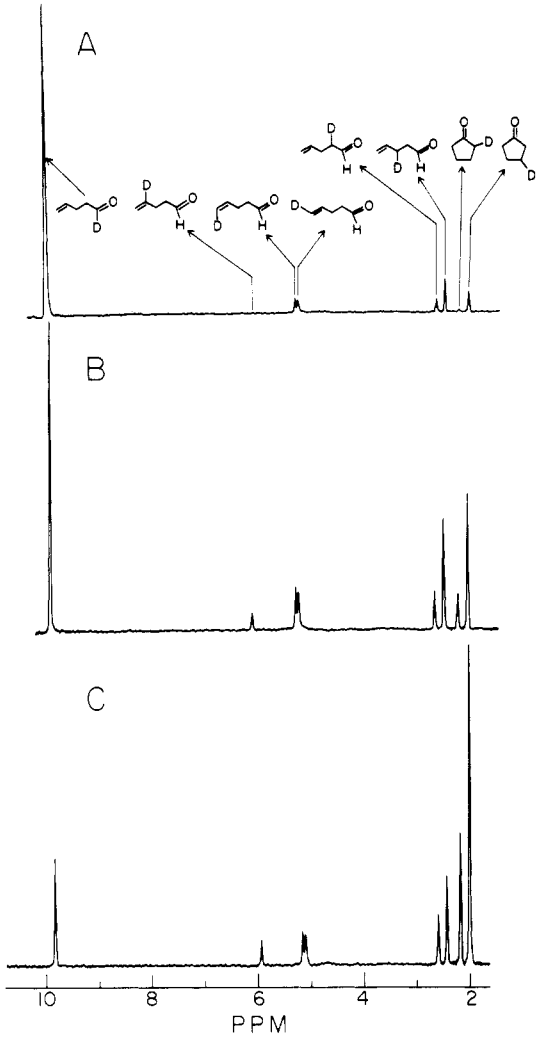

Figure 5. The observed deuterium scrambling of the CH_2=C-HCH_2CH_2CDO substrate using 1.0 mol % of the [Rh((*S,S*)-chiraphos)]$^+$ catalyst in CH_2Cl_2 solutions at 20 °C. The 61.4-MHz deuterium NMR spectra, from top to bottom, refer to 6.1%, 23.2%, and 56.6% conversions to cyclopentanone.

it not for the fact that cyclopentanones (**8** and **7**) are produced irreversibly from **2** and **5**. It is clear, however, that at no stage of catalysis is equilibrium reached between **1** and **13**. We infer this from the ratio **7**:**8** which varies during catalysis from about 20:1 to 2.7:1 at the end of catalysis. Since **7** is derived directly from **1** and **8** can only be derived from **5**, the preponderance of **7** early in the catalysis shows clearly that the hydroacylation process is faster than the equilibration of the species **2** ⇌ **4** ⇌ **5**. But the appearance of **13** shows that the equilibration of **1** ⇌ **13** is competitive with hydroacylation. Moreover, since the overall hydroacylation process is extremely rapid, C–H activation must also be a rapid but reversible process.

Transfer of deuterium to the terminal position **13**, however, is not the only deuterium scrambling that occurs. This was demonstrated by following the catalysis of the CH_2=$CHCH_2CH_2CDO$ substrate in CH_2Cl_2 solutions. We have used both the [Rh(diphos)]$^+$ catalyst and the analogous catalyst [Rh((*S,S*)-chiraphos)]$^+$ ((*S,S*)-chiraphos = $Ph_2PCH(CH_3)CH(CH_3)PPh_2$); the properties of the latter are given in the Experimental Section. The results for these two catalysts are qualitatively similar; the chiraphos catalyst has about one-half the turnover rate and generates more extensive scrambling of the deuterium. Figure 5 shows a series of ^2H NMR spectra at various stages of catalysis using the [Rh((*S,S*)-chiraphos)]$^+$ catalyst with 100

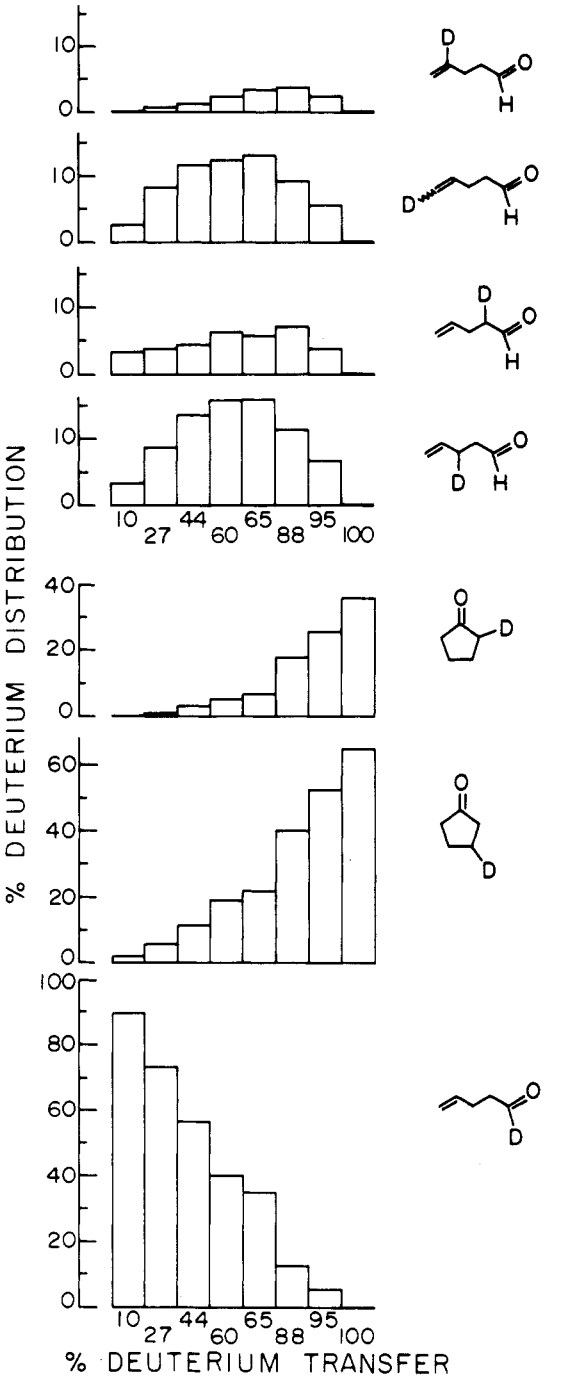

Figure 6. The concentration profiles of the various deuterated species observed during catalysis of the CH_2=$CHCH_2CH_2CDO$ with 1.0 mol % of the [Rh((*S,S*)-chiraphos)]$^+$ catalyst in CH_2Cl_2 solutions at 20 °C. The concentrations were measured by ^2H NMR.

equiv of the deuteriated CH_2=$CHCH_2CH_2CDO$ substrate in CH_2Cl_2 solutions at 20 °C. Remarkably, deuterium appears at every carbon atom of 4-pentenal during the course of catalysis. The concentration profiles for the appearance of deuterium at the various locations is shown in Figure 6.

The obvious way of distributing the deuterium among all of the carbon atoms from the CH_2=$CHCH_2CH_2CDO$ substrate is by first moving the deuterium to the 5-position (**13**) by the mechanism shown in Figure 4 followed by reversible double-bond migration via a π-allyl mechanism. This, however, cannot be the case because we find double-bond migration to be a much slower process[1] than the scrambling, and, furthermore, once the double bond has

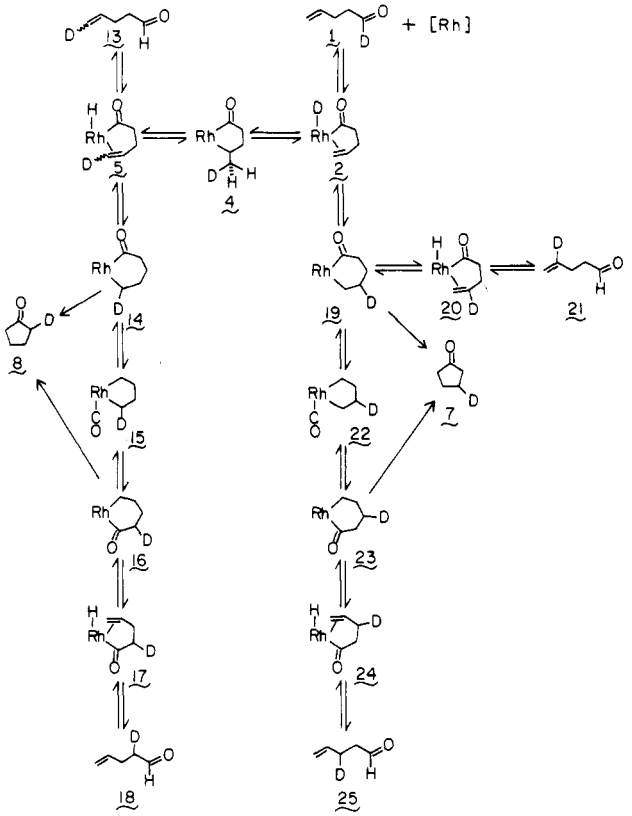

Figure 7. A detailed outline of the proposed mechanism of hydroacylation of 4-pentenal using the diphos and chiraphos catalysts. The positive charge of the rhodium species has been omitted, and all coordinatively unsaturated species shown in the diagram may contain either bound solvent or substrate molecules.

migrated, it remains at its new location. Were double-bond migration a reversible process we would expect that eventually all of the double-bond-migrated substrate would be "milked" back into the hydroacylation cycle. This does not happen. Moreover, if reversible double-bond migration were responsible for the extensive deuterium scrambling, we would expect to observe deuterium at the 3- and 4-positions of the substrate when the labeled, CH_2=CHC-H_2CD_2CHO, 4-pentenal was used. We do not. That irreversible double-bond migration occurs via the π-allyl mechanism for similar substrates and catalysts has been demonstrated before.[10] We have considered other, more exotic, mechanisms for deuterium scrambling, but none of these is consistent with the results. We conclude, therefore, that this remarkable deuterium scrambling is directly connected with the hydroacylation mechanism.

Mechanisms of Deuterium Scrambling

The implications of the deuterium scrambling for the hydroacylation mechanism are unusually complex, our interpretation of these results is outlined in Figure 7. The mechanism for delivering the deuterium to the 5-position **13** has been discussed (Figure 4), but the stereochemistry (E and Z) of the deuterium at the double bond of **13** is now known from ^2H NMR. Because the two hydrogen atoms of the monodeuteriated methyl group of **4** are diastereotopic, we might expect the (*S,S*)-chiraphos catalyst to abstract these protons (by β-elimination) at different rates. We find, however, no diastereoselection; the *E* and *Z* isomers of **13** are produced in equal proportions.

The mechanism for the appearance of the label at the 4-position **21** involves β-elimination of the six-membered metallacycle **19**. Six-membered metallacycles are known to β-eliminate[11] as we would expect in the present case because β-elimination is the microscopic reverse of the implied hydride-transfer process **2** → **19**.

The generation of deuterium at the 3-position **25** is assumed to occur via the steps **19** to **25**, a process that requires the carbonyl deinsertion of **19** to produce the five-membered metallacycle **22**. This species **22** can reinsert CO to the original end of the ring to give back **19** or into the other end of the ring to give **23** and thereby relocate the deuterium. Upon β-elimination, **23** gives **24** which reductively eliminates to produce 4-pentenal **25**, labeled at the 3-position.

The generation of the 2-position-labeled 4-pentenal **18** involves a similar but more circuitous path. First the deuterium is shifted to the 5-position via **4**, whereafter **5** collapses to **18** via the steps **14** to **18** which are totally analogous to those steps leading to **25**.

The mechanism outlined in Figure 7 is consistent with the results obtained by using the two other labeled substrates, CH_2=$CHC(CH_3)_2CH_2CDO$ and CH_2=$CHCH_2C$-D_2CHO. If the decarbonylated intermediates **15** and **22** do indeed form and the carbonyl can insert into either end of the metallacyclopentane, then the substrate CH_2=CH-CH_2CD_2CHO should generate CD_2=$CHCH_2CH_2CHO$ during catalysis. This is observed (see Experimental Section).

Similarly the CH_2=$CHC(CH_3)_2CH_2CDO$ substrate, while allowing the formation of the switched insertion intermediates **16** and **23**, will not allow for β-elimination to produce **17** or **24** because the requisite β-carbon atom is substituted by a *gem*-dimethyl group. Hence, the 3,3-dimethyl substituents of this labeled substrate block the paths leading to **18** and **25**. This substrate, however, does allow for the appearance of labels in the positions shown in **13** and **21**. The terminally labeled substrate **13** is observed for the *gem*-dimethyl substrate, but no label is observed at the 4-position **21** with either the diphos or chiraphos catalysts. We believe that 4-labeled substrate is produced, but its standing concentration is too low to measure by ^2H NMR. This assertion is probably true because no **21** is observed for the CH_2=$CHCH_2CH_2CDO$ substrate with the diphos catalyst; the analogous substrate CH_2=$CHCH_2CD_2CHO$ with the diphos catalyst gives CD_2=$CHCH_2CH_2CHO$ which is derived from steps (**22** to **25** or **15** to **18**) which include β-elimination of the six-membered metallacycle. The substrate **21** is also derived from the same β-elimination step (**19** to **21**).

It thus appears that the mechanism of hydroacylation of 4-pentenals using the [Rh(diphosphine)]$^+$ is credibly established by the deuterium scrambling observations. The extraordinary complexity of the mechanism is exemplified by the numerous reversible steps that can occur before the final irreversible act of reductive elimination to produce cyclopentanones. The hydroacylation process itself appears to be extraordinarily fast, and yet before hardly any cyclopentanone is produced, the deuterium scrambled substrates **13**, **21**, **18**, and **25** are observed with the chiraphos catalyst. A measure of the catalytic activity is given by the sum of the concentrations of **13**, **21**, **18**, **25**, **7**, and **8** although this is an underestimate since it does not measure the unobservable catalytic activity that regenerates **1** from **2**. Figure 8 shows plots of the catalytic activity

(10) Tani, K.; Yamagata, T.; Akutagawa, S.; Kimobayashi, H.; Taketomi, T.; Takaya, H.; Miyashita, A.; Noyori, R.; Otsuka, S. *J. Am. Chem. Soc.* **1984**, *106*, 5208.

(11) Yamamoto, T.; Sano, K.; Yamamoto, A. *J. Am. Chem. Soc.* **1987**, *109*, 1092.

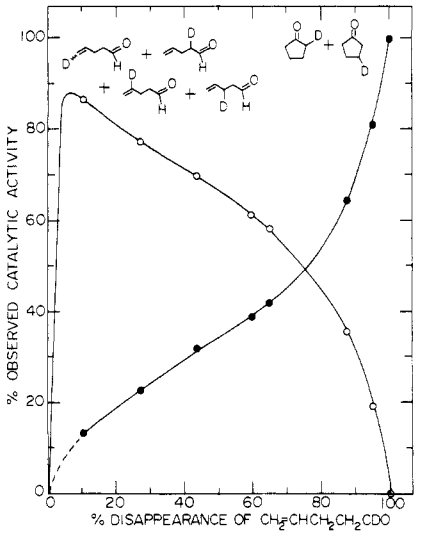

Figure 8. A plot of the observed total catalytic activity versus percent disappearance of $CH_2{=}CHCH_2CH_2CDO$ as measured by ^2H NMR for the hydroacylation of $CH_2{=}CHCH_2CH_2CDO$ with 1.0 mol% $[Rh((S,S)\text{-chiraphos})]^+$ catalyst in CH_2Cl_2 solutions at 20 °C.

that generates the deuterium-scrambled substrate and cyclopentanone versus extent of catalysis. It will be seen that at the beginning of the catalysis almost 90% of the catalytic activity generates deuteriated 4-pentenals and the remaining 10% leads to product.

From these plots it is apparent that oxidative addition (**1** → **2**), hydride transfer to the double bond (**2** → **19**), and all of the other steps are much faster than the reductive elimination which produces cyclopentanone (e.g., **19** → **7**). Hence the turnover limiting step of hydroacylation is the last step, the reductive elimination of the six-membered metallacycle. This last statement needs to be qualified by the recognition that the metallacyclohexanone **19** may be bound to a molecule of substrate and that the dissociation of the substrate may be turnover limiting. Whatever the case, the turnover limiting step is associated with a metallacyclohexanone intermediate.

We can now understand why the catalysis behaves as a "black box". Since the last step is turnover limiting, we might expect the 6-membered metallacycle (e.g., **19**) to build up in concentration under steady-state conditions and hence it might be possible to detect it. This, however, does not occur because all of the intermediates are continually being removed from the "black box" by fast reversible pathways, so that, at any time, the "black box" contains undetectable amounts of catalytic material. Because nearly all of the catalytic material lies outside the "black box" and yet the catalysis is rapid, the C–H oxidative addition step **1** → **2** must be very fast but its reverse **2** → **1** must be even faster. For hydroacylation to succeed at all requires that the C–H activation step occur many times before the material passes through the intermediates to a productive event. Moreover, since essentially all of the substrate resides outside the "black box", all of the reverse steps that drive the substrate out of the "box" are faster than the forward steps that lead to the production of cyclopentanone.

Substrate Decarbonylation

Substrate decarbonylation, although imortant in deactivating the catalyst, is generally a minor event in the hydroacylation mechanism. It could arise from the catalytic intermediates shown in Figure 9. The most obvious, and conventional, path for decarbonylation is via **26**. We,

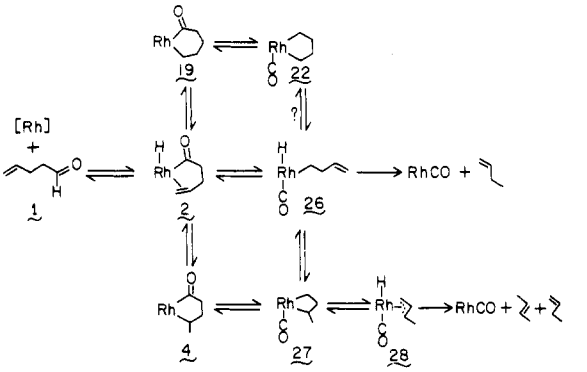

Figure 9. The possible pathways leading to decarbonylation of 4-pentenal by the $[Rh(diphosphine)]^+$ catalysts. The positive charge of the intermediates has been omitted, and all coordinatively unsaturated species shown in the diagram may contain either bound solvent or substrate molecules.

however, cannot exclude the other two paths involving β-elimination of the metallacyclobutane **27** or the metallacyclopentane **22**. There are examples of decomposition of metallacyclobutanes presumably via the π-allyl path shown,[12] and, perhaps surprisingly, certain metallacyclopentanes were shown to decompose, partly to butenes, under very mild conditions.[13] The putative path involving the metallacyclobutane **27** is unavailable to the 3,3-dimethyl-4-pentenal substrate because there are no hydrogen atoms at the endocyclic β-carbon atom of **27**. Decarbonylation does occur with this substrate but at a rate per unit turnover which is an order of magnitude less than that for any of the other substrates.

We have no firm evidence for deciding in favor of any of these three possible paths although we are inclined to prefer the process involving **2** → **26** because it is the simplest path. The fact that for most substrates decarbonylation is a minor process in the hydroacylation mechanism supports our earlier assertion[1] that the characteristics of the $[Rh(diphosphine)]^+$ catalysts would speed up the steps leading to cyclopentanones over those steps which lead to decarbonylation.

Discussion

The present study has demonstrated that hydroacylation with the [Rh(diphosphine)] catalysts is an unusually complex process. We find that substrate–catalyst interaction generates numerous adducts leading to substrate inhibition of catalysis. These substrate–catalyst adducts affect the turnover rate and turnover number, suggesting that the catalytic intermediates can be captured by a second substrate molecule such as the postulated intermediate **12**. Given this, it is possible that some of the numerous catalyst–adduct species observed during catalysis could be intermediates containing a second molecule of substrate which are pulled out of the catalytic cycle. We, however, were unable to identify any such species.

All of the steps, except the final reductive elimination to product, are fast and reversible. The reverse steps are much faster than the forward steps. The substrate, as it were, makes many attempts at surmounting the final turnover limiting step. Carbonyl deinsertion and reinsertion are both very rapid processes, but irreversible carbonylation of the catalyst is an infrequent event. We

(12) McQuillin, F. J.; Powell, K. C. *J. Chem. Soc., Dalton Trans.* **1972**, 2129.
(13) Lindner, E.; Jansen, R. M.; Meyer, H. A. *Angew. Chem., Int. Ed. Engl.* **1986**, *25*, 1008.

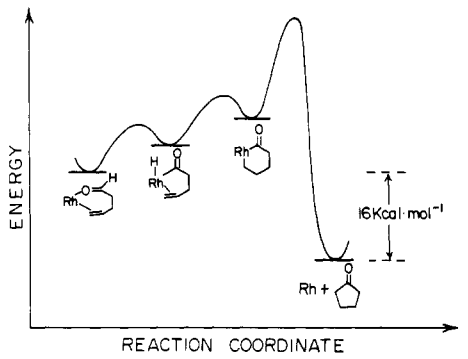

Figure 10. An estimated energy reaction profile for the main steps in the hydroacylation of 4-pentenal with the [Rh(diphos)]$^+$ catalyst. The positive charge of the intermediates has been omitted. The heat of formation of the reaction 4-pentenal to cyclopentanone is ~16 kcal mol^{-1}.

were unable to identify precisely the intermediate(s) leading to irreversible decarbonylation.

Figure 10 shows a semiquantitative reaction profile of the key steps in catalytic hydroacylation which, in outline, is consistent with present results. We note that the energy diagram implies that both C–H activation and hydride transfer to the olefin have low activation energies and that these two steps constitute a net endothermic process so that the reverse process, involving β-hydride elimination and acyl–hydride reductive elimination, is, as observed, kinetically and thermodynamically more favorable. The final step, the reductive elimination of the metallacyclohexanone, is allowed thermodynamically and has a significant kinetic barrier, and it controls the turnover rate of the catalysis. This implies that the reverse of the final step, C–C activation, is kinetically strongly unfavorable for these catalysts.

Figure 10 allows us to discuss the analogous, more general, reaction which we refer to as "hydrocarbonation", eq 2. Of the three primary steps of hydrocarbonation, C–H

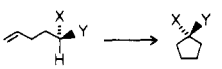

(2)

activation, olefin insertion into a metal–hydride bond, and reductive elimination of the metallacyclohexane, the second is expected to be rapid. One of the current views is that metal-induced C–H activation is a kinetically facile process,[14] and, if this is so, then the kinetic impediment to hydrocarbonation is the collapse of the metallocyclohexane to products. Although a known process,[15] the factors governing the rate of reductive elimination of metallacyclohexanes are not well understood except that probably for rhodium(III) metallacycles a complex with reduced coordination number is required.

With regard to C–H activation, the 1-pentene type substrates do have the advantage of anchoring the substrate by olefin coordination which will lead to rapid C–H activation through proximity effects. The most likely bond to be activated, however, is the one on the carbon α to the olefin leading to double-bond migration. We suppose, therefore, that one of the reasons that 4-pentenals generally undergo hydroacylation faster than double-bond migration is due to bidentate coordination via the aldehyde oxygen atom and the olefin group as in **10**. It may turn out that in order to accelerate hydrocarbonation over double-bond migration an additional weakly coordinating group is required so that the substrate can form a bidentate chelate to the catalyst. We should point out that the aldehyde C–H bond is considerably weaker (thermodynamically) than an aliphatic C–H bond (15–20 kcal mol^{-1}) and that this may be another reason for the success of hydroacylation. Despite all of the potential difficulties it seems to us that at present hydrocarbonation presents one of the more attractive methods for incorporating C–H bond activation in catalysis.

(14) Crabtree, R. H. *Chem. Rev.* **1985**, *85*, 245.
(15) Grubbs, R. H.; Miyashita, A. *J. Am. Chem. Soc.* **1978**, *100*, 7418.

Experimental Section

^{1}H, ^{2}H, ^{13}C, and ^{31}P NMR spectra were measured at 400, 61.4, 100.6, and 161.9 MHz, respectively, on a Varian XL-400 spectrometer. ^{1}H, ^{13}C, and ^{2}H NMR chemical shifts were recorded relative to TMS. ^{31}P NMR data were measured relative to an external reference (1% $P(OCH_3)_3$ in C_6H_6) but are reported relative to 85% H_3PO_4 (converted by adding 140.4 ppm). Low-temperature calibration was performed as reported.[16] Infrared spectra and gas chromatographs were obtained as noted.[1] [Rh(diphos)(PhBPh$_3$)],[7] [Rh(diphos)]$_2$(ClO$_4$)$_2$, 4-pentenal substrates, and solvents were obtained as previously reported.[1] Nitromethane was twice purified[17] and stored in the dark. Catalyses were performed as described.[1]

Substrate Synthesis. The percent of deuterium incorporation for each of the following three substrates was found to be >98% by ^{1}H NMR integration.

CH_2=CHCH$_2$CH$_2$CDO was prepared by reduction of 4-pentenoic acid with $LiAlD_4$ in diethyl ether followed by oxidation[18] of the resulting alcohol, CH_2=CHCH$_2$CH$_2$CD$_2$OH, with pyridinium chlorochromate in CH_2Cl_2. After filtration through Fluorosil/Celite, the product was purified by chromatography on Silica gel (eluent = 1:1 pentane/ether).

CH_2=CHCH$_2$CD$_2$CHO was synthesized from 4-pentenal[1] by pyridine-catalyzed exchange of the α-methylene protons in refluxing (17 H) D_2O. Chromatography as above and distillation led to 10% isolated yield.

CH_2=CHC(CH$_3$)$_2$CH$_2$CDO was obtained from 3,3-dimethyl-4-pentenal[1] through oxidation with Jones' reagent[19] to the corresponding acid (55% yield), followed as for CH_2=CHCH$_2$C-H$_2$CDO by $LiAlD_4$ reduction, reoxidation to the aldehyde with pyridinium chlorochromate[18] chromatography on Silica gel, and distillation (overall yield = 22%).

CH_2=CHCH$_2$CH$_2$COCH$_3$. The keto olefin was made by reaction of allyl bromide with the imine carbanion ($C_6H_{11}N$ = $C(CH_3)CH_2^-$) followed by hydrolysis of the resulting imine:[20] yield 13%; bp 70 °C (100 mm); ^{1}H NMR ($CDCl_3$) δ 5.4–6.2 (m, 1 H, =CH), 4.8–5.2 (m, 2 H, =CH$_2$), 2.2–27 (m, 4 H, CH$_2$), 2.18 (s, 3 H, CH$_3$).

Preparation of [Rh((*S*,*S*)-chiraphos)]$_2$(ClO$_4$)$_2$·CH$_3$OH. [Rh((*S*,*S*)-chiraphos)NBD]ClO$_4$ (^{31}P NMR (CD_3NO_2) δ 60.0 (J_{Rh-P} = 156 Hz)), synthesized from [Rh(NBD)$_2$]ClO$_4$ and (*S*,*S*)-chiraphos as reported for diphos,[1] was suspended in deoxygenated methanol (0.4 g in 2.0 mL), and H_2 was slowly bubbled through the stirring solution for 1.5 h. The now burgandy solution was treated with dry ($LiAlH_4$) deoxygenated diethyl ether to produce a yellow precipitate which was collected under Ar, washed (3 × 0.5 mL of ice-cold CH_3OH, 3 × 1.0 mL of ether) and dried under an Ar flow; isolated yield = 0.2 g (58%). Anal. Calcd for [Rh((*S*,*S*)-chiraphos)]$_2$(ClO$_4$)$_2$·CH$_3$OH ($Rh_2C_{57}H_{60}Cl_2P_4O_9$): C, 53.08; H, 4.66; Cl, 5.50; P, 9.61. Found: C, 50.27; H, 4.73; Cl, 5.46; P, 10.05. This complex is more soluble in CH_2Cl_2 than the diphos analogue (≥24 mg versus 2 mg/0.6 mL): ^{31}P NMR (CH_2Cl_2) δ 70.4 (J_{Rh-P} = 163 Hz); ^{31}P NMR (CH_3NO_2) δ_1 84.8 (J_{Rh-P} = 210 Hz, $J_{Rh'-P}$ = 9 Hz), 81.5 (J_{Rh-P} = 189 Hz), J_{P-P} = 49 Hz), δ_2 82.1 (J_{Rh-P} = 208 Hz, $J_{Rh'-P}$ = 9 Hz), 78.7 (J_{Rh-P} = 190 Hz), J_{P-P} = 49

(16) Dickert, F. L.; Hellmann, S. W. *Anal. Chem.* **1980**, *52*, 996. Vidrine, D. W.; Peterson, P. E. *Anal.* Chem. **1976**, *48*, 1301. Van Geet, A. *Anal. Chem.* **1970**, *42*, 679.
(17) Coetzee, J. F.; Chang, T. H. *Pure Appl. Chem.* **1986**, *58*, 1541.
(18) Novak, L.; Baan, G.; Marosfalvi, J.; Szantay, C. *Chem. Ber.* **1980**, *113*, 2939.
(19) Djerassi, C.; Engle, R. R.; Bowers, A. *J. Org. Chem.* **1956**, *21*, 1547.
(20) Larcheveque, M.; Valette, G.; Cuvigny, Th. *Tetrahedron*, **1979**, *35*, 1745.

Table I. Experimental Data for Effects of Varying Ratio ([Substrate]/[Rh]) and Specific Concentrations on Efficiency and Rate of Catalysis[a] of Cyclization of 4-Pentenal in Nitromethane

mol % of Rh[b]	[Rh], mM[c]	[S], mM[c]	[S]/[Rh]	[cyclopentanone]/[butene][d]	% conversn[e]
2.91[f]	9.8[g]	326	33	32	100
1.93[f]	10.2[g]	520	51	42	100
1.18[f]			84	56	98
1.17[f]	46.1	3950	86	57	98
0.89[f]	10.4[g]	1151	111	83	100
0.75[f]	18.2	2420	133	101	98
0.59[f]	13.0	2194	170	112	95
0.53[f]	3.4[h]	641	189	116	100
0.52[f]	10.2[g,h]	1934	190	123	86
0.50[f]	4.8[h]	953	197	122	95
0.37	10.0[g]	2705	271	97	71
0.23	9.7[g]	4245	436	77	41

[a] Using $[Rh(diphos)]_2(ClO_4)_2$. [b] mol of Rh/mol of 4-pentenal. [c] mol of Rh or S (= 4-pentenal)/volume solvent. [d] Gas chromatographic data. [e] % consumed 4-pentenal. [f] Conditions for Figure 3. [g] Conditions for kinetic plots in Figure 2. [h] Conditions of dilution experiment (see text).

Hz, δ_3 78.9 (J_{Rh-P} = 209 Hz, $J_{Rh'-P}$ = 9 Hz), 75.3 (J_{Rh-P} = 189 Hz), J_{P-P} = 48 Hz; Ratio of $\delta_1:\delta_2:\delta_3$ = 1.3:1.0:1.3.

These NMR data are consistent with $[Rh((S,S)\text{-chiraphos})]_2(ClO_4)_2$ existing as the monomer $[Rh((S,S\text{-chiraphos})ClO_4]$ in CH_2Cl_2 but as the dimer in three diastereomeric forms in CH_3NO_2. These different structures for the dimer are attributed to (R,R)-$[Rh((S,S)\text{-chiraphos})]_2^{2+}$, (S,S)-$[Rh((S,S)\text{-chiraphos})]_2^{2+}$, and (R,S)-$[Rh((S,S)\text{-chiraphos})]_2^{2+}$, arising because of the presence of the two chiral phosphorus atoms bound to bridging arene rings. In CD_3NO_2 the ^1H NMR spectrum shows numerous resonances in the 5–8 ppm region assignable bridging arene protons of the three dimers, while in CD_2Cl_2 this region is blank—these observations are consistent with the ^{31}P NMR results and the interpretation above.

Substrate Inhibition. Experimental data relating to the importance of specific concentrations as well as the ratio of [S]/[Rh] on the rate of catalysis (Figure 2) and product yield (Figure 3) are contained in Table I.

Catalyst Carbonylation. ^{31}P NMR data characterizing complexes of the catalyst with solvent, carbon monoxide, olefins, 4-pentenal, cyclopentanone, and a keto olefin are collected in Table II. The last entry represents a reaction intermediate observed at 0 °C and accounts for all of the rhodium except for some $[Rh(diphos)(CO)_2]^+$. It clearly has inequivalent phosphorus atoms and an unusually small J_{P-P} (= 8 Hz). No definite identification of this intermediate has yet been possible.

Deuterium Scrambling. The ^2H NMR chemical shifts (δ; CH_2Cl_2/TMS) for 4-pentenal deuteriated at the 1, 2, 3, 4, 5 (cis to H), and 5 (trans to H) positions and for the α- and β-deuteriated cyclopentanones are respectively 9.85, 2.60, 2.44, 5.96, 5.17, 5.12, 2.19, and 2.01.

During the course of catalysis in CH_2Cl_2 at 20 °C, deuterium scrambling was followed by ^2H NMR for each deuterium-labeled 4-pentenal (100 equiv) using the two catalysts $[Rh(diphos)]_2(ClO_4)_2$ (A) and $[Rh((S,S)\text{-chiraphos})]_2(ClO_4)_2$ (B), at 1.0 mol % rhodium.

CH_2=CHCH$_2$CD$_2$CHO. This substrate produced only CD_2=$CHCH_2CH_2CHO$ during its catalytic conversion to α-deuteriated cyclopentanone. The concentration of CD_2=$CHCH_2CH_2CHO$ reached a maximum after 60% disappearance of the starting substrate and amounted to 2.6% (A) and 6.3% (B) of the combined total deuterium distribution (starting substrate + scrambled substrate + cyclopentanone). These numbers represent the amount of deuterium scrambling occurring via CO deinsertion/reinsertion.

Similarly, at the same stage of reaction with A and B of CH_2=$CHCH_2CH_2CDO$, 2.7% and 6.3%, respectively, of the combined total deuterium appeared as CH_2=$CHCH_2CHDCHO$. In this case the deuterium label has to first scramble to the 5-position via the metallacyclopentanone (**1** → **2** → **4** → **5** → **13**, Figure 7), before shifting to the 2-position through CO deinsertion/reinsertion from the metallacyclohexanone (**13** → **18**, Figure 7).

Therefore the amount of CDH=$CHCH_2CH_2CHO$ produced from CH_2=$CHCH_2CH_2CDO$ with A and B, respectively (6.5% and 12.4%), after 60% disappearance of CH_2=$CHCH_2CH_2CDO$, consists of 2.7% (for A) and 6.3% (for B) from the CO deinsertion/reinsertion path (**5** → **14** → **15** → **16**, Figure 7) together with 3.8% and 6.1%, respectively, with A and B which arises directly from the metallacyclopentanone (**1** → **2** → **4** → **5** → **13**, Figure 7) without passing through the metallacyclohexanone (**14**, Figure 7).

CH_2=CHC(CH$_3$)$_2$CH$_2$CDO. For the reaction of this substrate with A or B, only CHD=$CHC(CH_3)_2CH_2CHO$ was observed during conversion to the α- and β-deuteriated cyclopentanones. The amount of CHD=$CHC(CH_3)_2CH_2CHO$ maximized after 60% transfer of deuterium from the starting substrate at 10.9% and 15.3% of the combined total deuterium with A and B, respectively.

CH_2=CHCH$_2$CH$_2$CDO. During catalysis with this substrate using $[Rh(diphos)]_2(ClO_4)_2$, deuterium was distributed among the 1-, 2-, 3-, 4-, and 5-positions of the substrate and α- and β-positions of cyclopentanones as 87:3.2:1.1:0:2.5:0.3:5.9% and later as 53:2.6:4.3:0:6.9:5.2:28.1%.

Table II. ^{31}P NMR Data for Complexes Formed from $[Rh(diphos)]_2(ClO_4)_2$ in CH_3NO_2

complex	δ (J_{Rh-P}, J_{P-P}, Hz)
$[Rh(diphos)]_2^{2+}$	81.5 (217, 36)[a]
	79.4 (196, 36)
$[Rh(diphos)(acetone)_2]^+$	81.2 (201)
$[Rh(diphos)(cyclopentanone)_2]^+$	81.5 (201)
$[Rh(diphos)(CO)(acetone)]^+$	75.6 (164, 34)[b,c]
	57.3 (131,34)
$[Rh(diphos)(CO)(cyclopentanone)]^+$	75.5 (168, 32)[b]
	57.4 (129, 32)
$[Rh(diphos)(CO)_2]^+$	65.6 (121)[d]
$[Rh(diphos)(pentene)_2]^+$	58.0 (157)
$[Rh(diphos)(NBD)]^+$	58.2 (157)
$[Rh(diphos)(5\text{-hexen-2-one})]^+$	80.4 (180, 34)[b]
	53.8 (165, 34)
$[Rh(diphos)(4\text{-pentenal})_n]^+$[e]	77.6 (143.8)
	68.9 (131, 8)

[a] Phosphorus trans to arene (major diastereomer). [b] Phosphorus trans to ketone. [c] IR $\nu_{C\equiv O}$ = 2011 cm^{-1}. [d] IR $\nu_{C\equiv O}$ = 2100, 2055 cm^{-1}. [e] Unidentified intermediate, accumulated at 0 °C after 1.5 h of reaction of 4-pentenal with 1.0 mol % of Rh as $[Rh(diphos)]_2^{2+}$, formed en route to $[Rh(diphos)(CO)_2]^+$. At this point <30% 4-pentenal was cyclized; the only other Rh species was 20% $[Rh(diphos)(CO)_2]^+$.

Registry No. *meso*-**9**, 112924-61-5; *racemic*-**9**, 112924-62-6; **10**, 112840-82-1; **11**, 109-49-9; $[Rh(diphos)(CO)_2]^+$, 74404-47-0; $[Rh(diphos)]^+$, 64867-96-5; $[Rh(diphos)(CO)(acetone)]^+$, 112840-74-1; $[Rh(diphos)(CO)(cyclopentanone)]^+$, 112840-75-2; D_2, 7782-39-0; $[Rh((S,S\text{-chiraphos})]^+$, 112840-76-3; CH_2=$CHCH_2CH_2CDO$, 112840-83-2; CH_2=$CHCH_2CD_2CHO$, 18932-26-8; CH_2=$CHC(CH_3)_2CH_2CDO$, 112840-84-3; CH_2=$CHCH_2CH_2COCH_3$, 109-49-9; $C_6H_{11}N$=$C(CH_3)CH_2^-$, 112840-85-4; (R,R)-$[Rh((S,S)\text{-chiraphos})]_2(ClO_4)_2$, 112840-78-5; $[Rh((S,S)\text{-chiraphos})NBD]ClO_4$, 65012-74-0; $[Rh(NBD)_2]ClO_4$, 60576-58-1; (S,S)-chiraphos, 64896-28-2; (S,S)-$[Rh((S,S)\text{-chiraphos})]_2(ClO_4)_2$, 112924-64-8; (R,S)-$[Rh((S,S)\text{-chiraphos})]_2(ClO_4)_2$, 112924-66-0; $[Rh(diphos)(acetone)_2]^+$, 88821-69-6; $[Rh(diphos)(cyclopentanone)_2]^+$, 112840-79-6; $[Rh(diphos)(pentene)_2]^+$, 112840-80-9; $[Rh(diphos)(5\text{-hexen-2-one})]^+$, 112840-81-0; 4-pentenal, 2100-17-6; 1-pentene, 109-67-1; cyclopentanone, 120-92-3; 4-pentenoic acid, 591-80-0; 3,3-dimethyl-4-pentenal, 919-93-7; 3,3-dimethyl-4-pentenoic acid, 7796-73-8; allyl bromide, 106-95-6.